Peer-reviewed version available at *Atoms* **2018**, *6*, 46; doi:10.3390/atoms6030046

Research Article

Plasma expansion dynamics in ultra-high-pure hydrogen gas

Ghaneshwar Gautam [1], and Christian G. Parigger [2,*]

[1] Fort Peck Community College, 605 Indian Avenue, Poplar, MT - 59255; ggautam@fpcc.edu
[2] Department of Physics and Astronomy, University of Tennessee/University of Tennessee Space Institute, 411 B. H. Goethert Parkway, Tullahoma, TN - 37388; cparigge@tennessee.edu
* Correspondence: cparigge@tennessee.edu; Tel.: +1-931-841-5690

Abstract: Micro-plasma is generated in ultra-high-pure hydrogen gas filled inside a cell at a pressure of (1.08 ± 0.033) × 10^5 Pa (810 ± 25 Torr) by using a Q-switched Nd:YAG laser device operated at 1064 nm wavelength and 14 ns pulse duration. Micro-plasma emission spectra of the hydrogen Balmer alpha line, H_α, are recorded with a Czerny-Turner type spectrometer and an intensified charge-coupled device. The spectra are calibrated for wavelength and corrected for detector sensitivity. During the first few tens of nanoseconds after initiating optical breakdown, significantly Stark-broadened and Stark-shifted H_α lines mark the well-above hypersonic outward expansion. The vertical diameters of the spectrally resolved plasma images are measured for time delays of 10 ns to 35 ns to determine expansion speeds of the order of 100 km/s to 10 km/s. For time delays of the order of 0.5 µs to 1 µs, the expansion decreases to the speed of sound of 1.3 km/s in the near ambient temperature and pressure hydrogen gas.

Keywords: Laser-plasma interactions; Plasma dynamics and flow; Hypersonic flows; Emission Spectra

1. Introduction

In laser-induced plasma, the ambient gas can foster or diminish the plasma expansion. Pressure and types of gases also influence post-breakdown phenomena. For example, at low pressure, the losses and uniformity of the plasma energy distribution increases [1]. Plasma size, propagation speed, and emission property are also related to the ambient gas into which the plasma expands. Here, we focus on the determination of the expansion speed of the micro-plasma generated in the ultra-high-pure (UHP) hydrogen gas inside a cell. Experimental result shows high plasma expansion speeds of 100 km/s to 10 km/s at early time delays of 10 ns to 35 ns. The physical cause of this high speed is the large pressure difference between the plasma and its surrounding environment. The high expansion speed decreases continuously as the time delays increase. Study of the plasma expansion is applicable for astrophysical, engineering, scientific research as well as other various applications [2, 3, 4].

During the plasma expansion, spatial and temporal variations of density, temperature and pressure are observed. Investigation of these spatial and temporal profiles allow us to infer the expansion speeds. Plasma at elevated temperature and pressure expands with high velocity and drives the shock wave into outward direction to release the high pressure. Figures 1 to 3 display the recorded H_α plasma spectra at early time delays of 10 ns to 35 ns in 5 ns steps. The 2-dimensional spectra of slit-height versus wavelength are significantly Stark-broadened and Stark-shifted at early time delays. The measured intensity is increasing for successive time delays. However, the area under the spectral profiles decreases continuously due to the decrease of the line widths, consistent with decreasing electron density. If the incident laser beam is focused to above breakdown threshold irradiance, breakdown occurs at a location before the pulse reaches its focal point, as indicated in

Preprints (www.preprints.org) | NOT PEER-REVIEWED | Posted: 13 July 2018 doi:10.20944/preprints201807.0229.v1

Peer-reviewed version available at Atoms 2018, 6, 46; doi:10.3390/atoms6030046

Figure 5 of Reference [5]. This type of behavior is also observed in the hydrogen experiments reported in this work.

The interaction between the laser beam and material is a complex process, and depends on many characteristics such as laser parameters or target material. Various factors affect the interaction including the properties such as the pulse width, spatial and temporal fluctuation of the pulse as well as the peak irradiance variations. For example, effects of pulse width on nascent laser-induced bubbles for underwater laser-induced breakdown spectroscopy (LIBS) show that a long pulse causes well-defined, clear line spectra. In turn, a short pulse usually causes considerably asymmetric or deformed spectra. However, this effect is more significant for solid target material than for gases [6].

2. Results

From the recorded H_α plasma spectra at early time delay as displayed in Figures 1 – 3, plasma expansion speeds are determined. The diameter of the plasma in the lateral or slit-height direction is measured as a function of time, and hence plasma expansion speed can be determined. For example, the red arrows on the spectra images at 10 ns and 15 ns in Figure 1 indicates the spatial plasma ranges used for the determination of the expansion speeds.

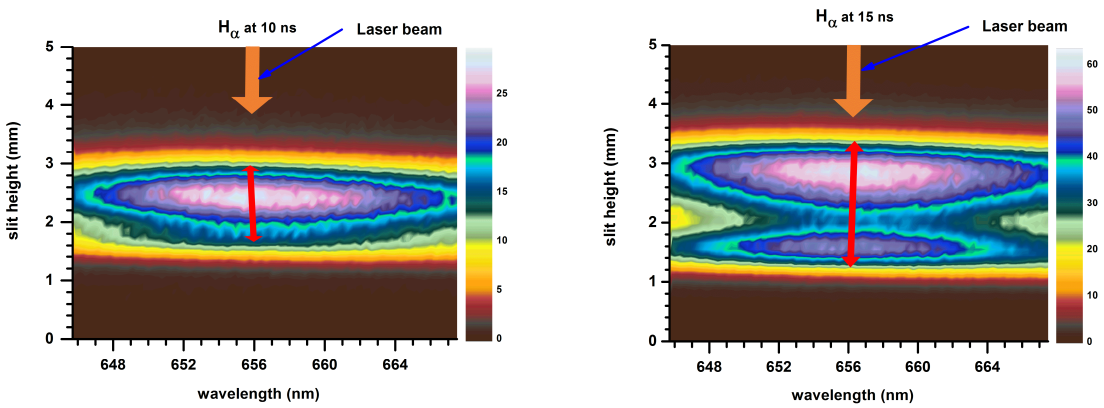

Figure 1. Hydrogen alpha plasma spectra images at 10 ns (left) and 15 ns (right) time delays. The red arrow indicates the measured plasma width.

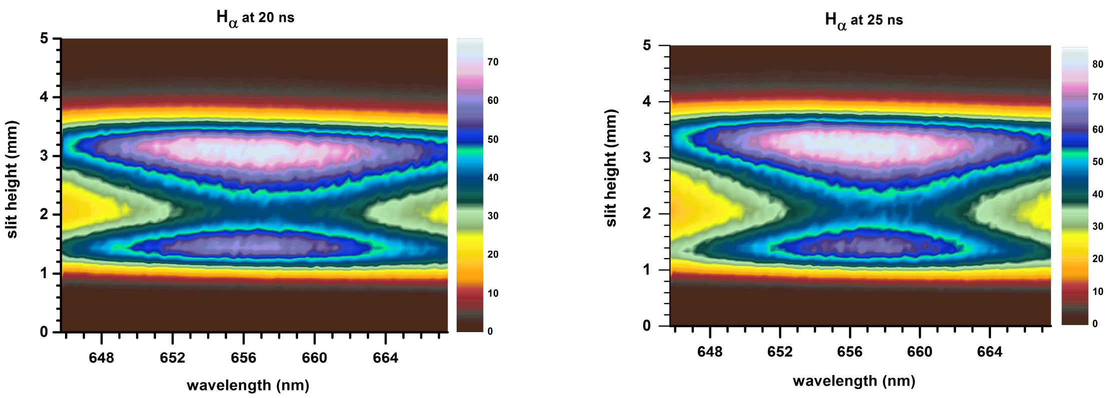

Figure 2. Hydrogen alpha plasma spectra images at 20 ns (left) and 25 ns (right) time delays.

Preprints (www.preprints.org) | NOT PEER-REVIEWED | Posted: 13 July 2018 doi:10.20944/preprints201807.0229.v1

Peer-reviewed version available at Atoms 2018, 6, 46; doi:10.3390/atoms6030046

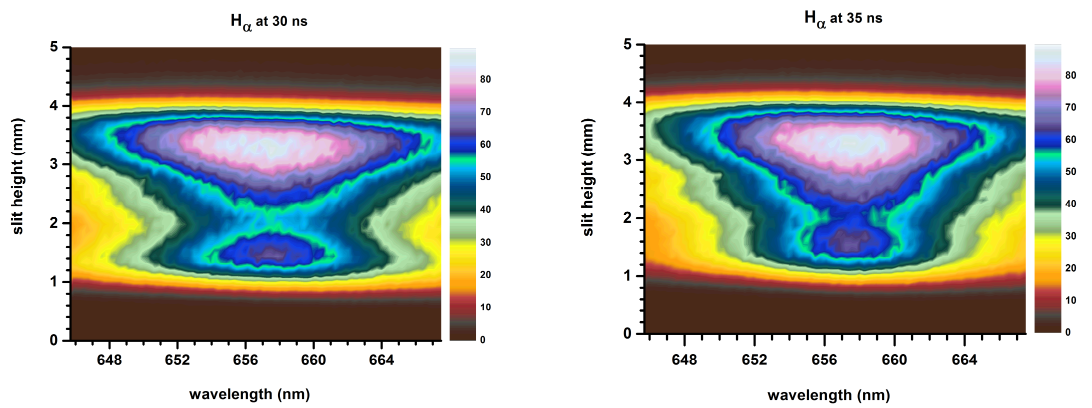

Figure 3. Hydrogen alpha plasma spectra images at 30 ns (left) and 35 ns (right) time delays.

The recorded images of the laser-induced plasma with 14 ns pulses depict higher intensity towards the laser at early time delay of 10 ns to 35 ns. On the other hand, previous experiment performed in hydrogen gas at 1.08 × 10^5 Pa (810 Torr) pressure with 6 ns pulse duration show higher intensity away from the laser propagation direction, for time delays of 12 ns and 30 ns. Opposite behavior occurs for a time delay of 300 ns [7]. This opposite behavior at later time delay is also observed in the experimental records as displayed in Figure 4.

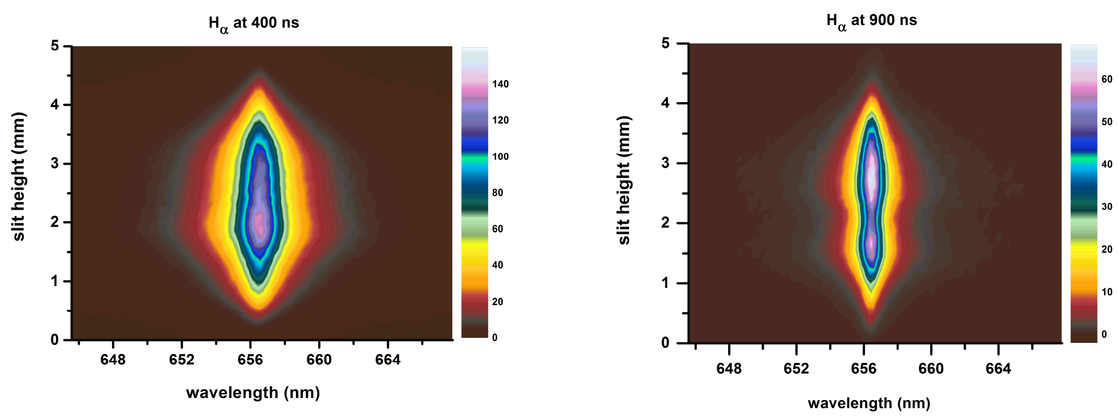

Figure 4. Hydrogen alpha plasma spectra images at 400 ns (left) and 900 ns (right) time delays.

In comparison, the experimental results in air, using Nd:YAG laser at the wavelength of 532 nm and pulse width of 6.5 ns, show two distinct regions with higher intensity towards the laser propagation direction for time delays of 25 ns to 10 μs, see Figure 8 in Reference [8]. Schlieren images of the laser-induced plasma generated in air at standard ambient temperature and pressure also show the jet propagation towards the laser for time delays of 1 μs to 20 μs [9]. However, the jet propagation direction depends on the type of gas and its pressure as displayed in Figure 3 in Reference [9]. Furthermore, the jet propagation depends on the ratio of energy absorbed in the plasma and threshold irradiance for optical breakdown [9].

Preprints (www.preprints.org) | NOT PEER-REVIEWED | Posted: 13 July 2018 doi:10.20944/preprints201807.0229.v1

Peer-reviewed version available at Atoms 2018, 6, 46; doi:10.3390/atoms6030046

From the images in Figures 1 to 3, the diameter of the plasma in lateral or slit height direction is measured as a function of time, and hence plasma expansion speeds can be diagnosed. The measured diameters of the plasma and corresponding speeds at various time delays are displayed in Table 1.

Table 1. Plasma expansion speed at various time delay using lateral direction expansion from the contour plots exhibited in Figures (1 – 4).

Time (ns)	Diameter (mm)	Distance in 5 ns (mm)	Speed (km/s)
10	1.32	--	--
15	2.03	0.71	142
20	2.42	0.39	78
25	2.71	0.29	58
30	2.86	0.15	30
35	2.92	0.06	12
400	0.96	--	--
900	1.81	0.85*	1.70

*Distance is for 500 ns.

The predicted plasma expansion speeds are of the order of 100 to 10 km/s at the indicated time delays. The determined expansion speeds are well-above hypersonic speed (Mach number ≥ 5) or above re-entry speeds (Mach number ≤ 25) at these time delays, as displayed in Figure 5.

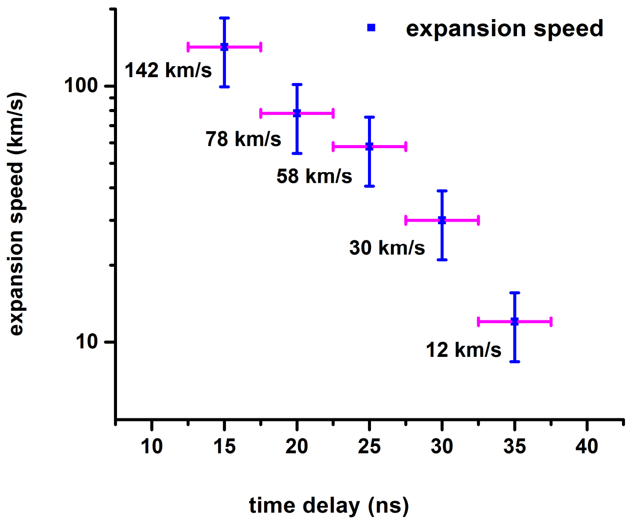

Figure 5. Plasma expansion speeds in log scale (see Table 1). The indicated time-delay error bars are due to the gate width of 5 ns.

The speed decreases to typically hypersonic speed for larger time delays than indicated in Figure 5. The predicted expansion speeds agree with results from previous experiments [9, 10]. Computer simulations show a shock wave expansion speed of 60 km/s at a time delay of 20 ns in air and at atmosphere pressure [11], thereby indicating that the determined speeds are in agreement with other experiments as well. The notable point here is that speed of sound in hydrogen gas is 1.3 km/s, a factor of 3.5 higher than in air. For later time delays of about 1 μs, the images in Figure 4 are utilized for the diagnostics of the plasma expansion speed. The determined speed is 1.7 ± 0.5 km/s at 900 ns. This result appears reasonable when comparing to the results of the recent hydrogen experiments [12]. The estimated error bars for these speeds are ± 30%.

3. Discussion

The laser-induced plasma expands with well-above hypersonic speed depending upon the ambient conditions and time delays. The spectra recorded during the evolution of the plasma are significantly Stark-broadened and Stark-shifted, therefore, a larger percentage error occurs for the predicted speeds for earlier time delays. For later time delays, plasma expansion speeds decrease considerably, therefore, larger differences occur for the speed measurement due to the increased temporal interval. To improve the graphically inferred expansion speeds, Abel inversion methods can be applied so that radial information will be extracted from the recorded line-of-sight measurements [13]. The predicted expansion speeds may be useful for the NASA hypersonic technology (HT) project. Hydrogen redshifts of hydrogen alpha and hydrogen beta lines are applicable in the study of white dwarfs [14]. Details of the focal volume irradiance distribution [15] for the study of laser-induced optical breakdown may augment the analysis.

4. Materials and Methods

In the experimental arrangement, ultra-high-pure (UHP) hydrogen gas is filled inside a cell at pressure of $(1.08 \pm 0.033) \times 10^5$ Pa (810 ± 25 Torr). To study time-resolved and space-resolved emission spectroscopy, a Q-switched Nd:YAG laser device is used at its fundamental wavelength of 1064 nm with 10 Hz repetition rate and 14 ns full-width-half-maximum pulses. The measured energy per pulse is 120 mJ. The laser beam was passed through a dichroic beam splitter to remove the residual 532 nm component. A silicon photodiode detector was used to record a portion of the laser radiation reflected off of the beam splitter at the exit of the laser source. The photodiode is connected to the oscilloscope to monitor the optical pulse. Three mirrors (NB1-K13; Thorlabs) are used to align the beam parallel to the spectrometer slit. A holographic grating of 1200 grooves/mm is selected to disperse the radiation from the plasma. For the recording of temporally and spatially resolved plasma emission spectra images along the slit height, the following instrumentation is employed: Czerny-Turner type spectrometer (0.64 m - HR640; Jobin-Yvon) and 2-dimensional integrated charged coupled device (ICCD) (Andor technology model iStar). The spectral resolution amounted to 0.11 nm. The data were recorded with a 5 ns gate width and an average of 100 consecutive laser-plasma events were accumulated. For later time delays of 400 ns and 900 ns, 20 ns gate width and 50 consecutive laser-plasma events were accumulated. The recorded spectra are wavelength calibrated and corrected for detector sensitivity.

5. Conclusions

Optical breakdown is induced by using pulsed laser radiation. Emission spectra are collected by employing a spectrometer equipped with an intensified charge-coupled device. Laser-induced micro-plasma dynamics are investigated in ultra-high-pure hydrogen gas focusing on atomic spectroscopy of hydrogen in the visible region. Line-of-sight measurements are analyzed to obtain the plasma dynamics that occur initially well-above re-entry speeds, diminish to hypersonic, and then supersonic expansions. Expansion velocities are measured that are above three hundred times the speed of sound in standard atmosphere. The recorded spectra can also be utilized to explore the spatial distributions of electron densities and excitation temperatures.

Author Contributions: Christian G. Parigger and Ghaneshwar Gautam designed and performed the experiments. Ghaneshwar Gautam analyzed the result and wrote the paper with suggestions from Christian G. Parigger.

Acknowledgments: This work is in part supported by the Center of excellence for Laser Applications at The University of Tennessee Space Institute.

Conflicts of Interest: The authors declare no conflict of interest.

References

1. Anabitarte, F., Cobo, A., and Lopez-Higuera, J.M. Laser-induced breakdown spectroscopy: fundamentals, applications, and challenges. *International Scholarly Research Notes: Spectroscopy* **2012**, doi: doi:10.5402/2012/285240.
2. Falcon, R.E., Rochau G.A., Bailey, J.E., Ellis, J.L., Carlson, A.L., Gomez, T.A., Montgomery, M.H., Winget, D.E., Chen, E.Y., Gomez, M.R., Nash, T.J. An experimental platform for creating white dwarf photospheres in the laboratory. *High Energy Density Physics* **2013** 9, pp. 82-90, doi: https://doi.org/10.1016/j.hedp.2012.10.005.
3. Falcon, R.E, Rochau, G.A., Bailey, J.E., Gomez, T.A., Montgomery, M.H., Winget, D.E., and T. Nagayama, T. Laboratory measurements of white dwarf photospheric spectral lines: H_β. *Astrophy. J.* **2015**, 806:214, 11 pp., doi: https://doi.org/10.1088/0004-637X/806/2/214.
4. Engeln, R., Mazouffre, S., Vankan, P., Bakker, I., Schram, D.C. Plasma expansion: fundamentals and applications. *Plasma Sources Science Technology* **2002**, 11, pp. A100, doi: https://doi.org/10.1088/0963-0252/11/3A/315.
5. Chen, Y.L., Lewis, J.W.L., and Parigger, C.G. Spatial and temporal profiles of pulsed laser-induced air plasma emissions. *J. Quant. Spectrosc. Radiat. Transfer* **2000**, 67, pp. 91-103, doi: https://doi.org/10.1016/S0022-4073(99)00196-X.
6. Sakka, T., Tamura, A., Matsumoto, A., Fukami, K., Nishi, N., and Thornton, B. Effects of pulse width on nascent width on nascent laser-induced bubbles for underwater laser-induced breakdown spectroscopy. *Spectrochim. Acta Part B: At. Spectrosc.* **2014**, 97, pp. 94-98, doi: https://doi.org/10.1016/j.sab.2014.05.009.
7. Glumac, N., Elliott, G. and Boguszko, M. Temporal and spatial evolution of a laser spark in air. *AIAA Journal* **2005**, 34, pp. 1984-1994, https://doi.org/10.2514/1.14886.
8. Brieschenk, S., O'Byrne, S. and Kleine, H. Visualization of jet development in laser-induced plasmas, *Opt. Lett.* **2013**, 38, pp. 664-666, doi: https://doi.org/10.1364/OL.38.000664.
9. Parigger, C.G., Plemmons, D. H., and Lewis, J.W.L. Spatially and temporally resolved electron number density measurements in a decaying laser-induced plasma using hydrogen-alpha line profiles. *Appl. Opt.* **1995**, 34, pp. 3325-3330, doi: https://doi.org/10.1364/AO.34.003325.
10. Parigger, C.G. Atomic and molecular emissions in laser-induced breakdown spectroscopy. *Spectrochim. Acta Part B: At. Spectrosc.* **2013**, 79, pp. 4-16, doi: https://doi.org/10.1016/j.sab.2012.11.012.
11. Sobral, H., Villagrán-Muniz, M., Navarro-González, R., and Raga, A. C. Temporal evolution of the shock wave and hot core air in laser induced plasma. *Appl. Phys. Lett.* **2000**, 77, pp. 3158-3160, doi: https://doi.org/10.1063/1.1324986.
12. Parigger, C. G., Surmick, D. M., and Gautam, G. Self-absorption characteristics of measured laser-induced plasma line shapes. *J. Phys.: Conf. Ser.* **2017** 810, pp. 012012, doi: https://doi.org/10.1088/1742-6596/810/1/012012.
13. Parigger, C. G., Gautam, G., and Surmick, D. M. Radial electron density measurements in laser-induced plasma from Abel inverted hydrogen Balmer beta line profiles. *Int. Rev. At. Mol. Phys.* **2015**, 6, pp. 43-55.
14. Parigger, C.G., Drake, K.A., Helstern, C.M., Gautam, G. Laboratory Hydrogen-Beta Emission Spectroscopy for Analysis of Astrophysical White Dwarf Spectra. At*oms* **2018**, 6, pp. 33–49. doi: https://doi.org/10.3390/atoms6030036.
15. Parigger, C.G. Laser-induced breakdown in gases: Experiments and simulation. In *Laser-induced breakdown spectroscopy*. Miziolek, A. W., Palleschi, V., and Schechter, I., Eds. Cambridge University Press, **2006**.